Current Applied Science and Technology Vol. 23 No. 2 (March-April 2023)

Research article

Peroxydisulfate Co-Treatment with MnOx-Loaded Biochar for COD Removal from Automobile Service Station Wastewater

Glinsukol Suwannarat, Kunlasatree Pattanagulanan, Chonlada Rueangsukhon, Panatda Nasingthong and Chompoonut Chaiyaraksa*

Environmental Chemistry Program, Department of Chemistry, School of Science, King Mongkut's Institute of Technology Ladkrabang, Bangkok, Thailand

Received: 17 May 2022, Revised: 6 July 2022, Accepted: 9 August 2022

DOI: 10.55003/cast.2022.02.23.004

Abstract

Keywords

biochar;

corn cob;

manganese oxide;

oxidation;

sodium peroxydisulfate

This research was aimed at recycling agricultural waste and treating synthetic automobile service station wastewater. Wastewater was synthesized to two levels of COD concentration: 702 mg/L (WW-A) and 7,054 mg/L (WW-B). In the treatment process, 100 mM sodium peroxydisulfate with MnO_x-loaded biochar (MnO_x-Biochar) was applied. The MnO_x-Biochar was produced by dipping corn cob biochar in 40 mM manganese sulfate followed by pyrolyzed at 600°C. The surface area, pore volume, pore size, and pH value at the zero-point charge of MnO_x-Biochar were 130 m^2/g, 0.044 cm^3/g, 1.02 nm, and 7.05, respectively. From the FTIR spectrogram, a peak assignable to Mn-O was observed. The results showed that the initial pH of the wastewater did not affect the treatment efficiency. The optimum MnO_x-Biochar dosage was 2 g/L. Equilibrium was reached within 120 min of reaction. During the first 15 min, the treatment rate constants (k) of the WW-A and WW-B treatment were 0.0647 min^{-1} and 0.0349 min^{-1}, respectively. After 15 min, the k values of the WW-A and WW-B treatments were reduced to 0.0242 min^{-1} and 0.0094 min^{-1}, respectively. The overall treatment efficiencies of the low COD wastewater (WW-A) and high COD wastewater (WW-B) were 97% and 78%, respectively. The treatment mechanisms involved both adsorption and oxidation. The adsorption efficiencies of the WW-A and WW-B treatments were 36% and 18%, respectively.

*Corresponding author: Tel.: (+66) 971929905 Fax: (+66) 23298428
E-mail: kcchompoonut@gmail.com

1. Introduction

Significant environmental pollution in Thailand, such as wastewater, is one of the country's top problems that must be addressed in order to improve people's quality of life. Currently, Thailand is an agriculture-based country that generates a lot of agricultural waste that can be recycled. In 2021, 8.38 million tons of corn were produced in the country, and this involved the generation of a large volume of corn cob waste [1]. Corn cob waste can be modified to add value. Researchers converted agricultural waste to biochar and used it to treat wastewater [2]. Wastewater from automobile service stations is one wastewater source that has not been seriously considered. Thailand currently has about 28,210 automobile service stations [3]. The effluent from the stations has high total solids (110-6,262 mg/L), COD (2.18-20,781 mg/L), oil and grease (14-420 mg/L), including various kinds of heavy metals (Cu, Cr, Pb, Zn, Al, Ni, Cd, Mn, As) [4]. When the wastewater is discharged into the water sources, floating oil residues obstruct light transmission into the water source. The water becomes spoiled, cannot be used, and various benthic macroinvertebrate assemblages are adversely affected [5]. Various techniques such as electrocoagulation [6], ultrafiltration [7], microfiltration, reverse osmosis [8], bioremediation [9], and oxidation [10] have been studied in the treatment of wastewater from automobiles and vehicle wash service stations. Over the last decade, advanced oxidation processes (AOPs), such as oxidation by O_3, O_3/H_2O_2, UV, UV/O_3, UV/H_2O_2, $O_3/UV/H_2O_2$, Fe^{2+}/H_2O_2 [11, 12], have been widely applied for wastewater treatment. Metal ions or metal oxides were applied as process catalysts [13-16]. In these processes, highly reactive and nonselective hydroxyl radical were generated. Later, sulfate radicals were included in the oxidative processes. Researchers reported that sulfate radicals were more effective at oxidizing than hydroxyl radicals. The redox potential of persulfate radicals is higher than hydroxyl radicals [17, 18].

More powerful sulfate radicals can be formed by various activation methods, including heat, UV, alkali, and the addition of metal oxides (nickel oxide, aluminum oxide, titanium oxide, cerium oxide, zero-valent iron, and manganese oxide) [19-22]. Manganese oxide is available naturally with low cost. The excellent properties of manganese oxide, such as its various Mn valences and low toxicity, make it interesting for use as a catalyst [23]. Carbon-based materials such as activated carbon and biochar can act as electron donors for persulfate to form sulfate radicals [24]. Biochar modified with manganese oxide was successfully applied to increase the persulfate oxidation efficiency [25]. In addition to being used as catalysts, manganese oxide and biochar were also employed as pollutant adsorbents. Faheem *et al.* [26] increased water pollution adsorption efficiency using manganese oxide-loaded biochar.

As mentioned above, manganese oxide-loaded biochar has been used for different purposes, but studies on integrated treatment mechanisms for organic waste removal are limited. In this study, we focused on the performance of catalytic oxidation of organic matter using MnO_x-loaded biochar to activate peroxydisulfate in a batch environment. Herein, the effect of some operating parameters on the efficiency of the process and oxidation kinetics have been evaluated and then discussed. The adsorption kinetics of MnO_x-loaded biochar were also studied and reported.

2. Materials and Methods

2.1 Materials

Ferrous ammonium sulfate, sulfuric acid, potassium dichromate, potassium hydrogen phthalate, silver sulfate, mercury sulfate, nitric acid, and sodium hydroxide were purchased from Carlo Erba. Sodium peroxydisulfate was supplied by Sigma-Aldrich. Manganese sulfate was purchased from Loba Chamie. All chemicals were of analytical grade.

2.2 Synthetic wastewater preparation

High COD synthetic wastewater (WW-B) was synthesized by adding 2 mL of used lubricant obtained from an automobile service station and 1 mL of surfactant solution (Sunlight) to 1 L of distilled water. Low COD concentration wastewater (WW-A) was synthesized by diluting WW-B 10 times. COD concentration was determined by titrimetric method [27].

2.3 Biochar and manganese oxide-loaded biochar (MnO_x-Biochar) preparation

Using a modified method from Fan *et al.* [25], corn cob was first cleaned with tap water, chopped into small pieces, dried at 100°C for 24 h in an oven, and pyrolyzed at 400°C for 4 h without oxygen. The produced biochar was then crushed to pass through a 35-mesh sieve. The production of manganese oxide-loaded biochar (MnO_x-Biochar) was done by adding 20 g of powdered biochar to 1 L of 40 mM manganese sulfate solution. The solution was agitated at 120 rpm for 2 h, and then filtered. The solid particles were dried at 100°C for 24 h, pyrolyzed at 600°C for 30 min, washed with double distilled water, and finally dried at 60°C for 24 h.

2.4 Biochar and manganese oxide-loaded biochar (MnO_x-Biochar) characterization

A Fourier Transform Infrared Spectrometer (FTIR; Perkin Elmer model spectrum GX) with KBr pellet sample preparation technique was applied to determine the surface structural groups. An atomic adsorption spectrophotometer (AAS; Perkin Elmer model AAS200) with acid digestion preparation technique was used to analyze the Mn composition of the biochar and MnO_x-Biochar [28]. A Brunauer Emmett Teller (BET)/gas adsorption analyser was utilized to determine the pore volume, pore size, and surface area of the biochar and MnO_x-Biochar. The pH value at the zero-point charge of MnO_x-Biochar was determined by preparing a 0.01 M NaCl solution at various pHs, adding an adsorbent, measuring the solution pH after shaking for 24 h, and plotting the graph between the initial and final pH [29].

2.5 Treatment process

The initial pH of 50 mL synthetic wastewater was adjusted with 0.1 M HCl or 0.1 M NaOH. Sodium peroxydisulfate (1.19 g) was added to obtain the concentration of 100 mM. After adding a certain amount of MnO_x-Biochar, the solution was agitated at 120 rpm for various periods and then filtered through 0.42 µm filter paper. After treatment, the COD of the solutions was determined. Mn leaching in wastewater after treatment was tested using AAS. All experiments were performed in triplicate. Treatment kinetics was calculated following the pseudo-first-order kinetic model as shown in equation (1) [15]:

$$ln\frac{C_t}{C_0} = -kt \quad (1)$$

C_t = the COD concentration in solution at time t (mg/L)
C_0 = the COD concentration in solution at time 0 (mg/L)
t = time (min)
k = the rate constant for pseudo-first order (1/min)

2.6 Adsorption process

The experimental procedure was the same as Section 2.5, except that sodium peroxydisulfate was not added. Adsorption kinetics were calculated using equations (2) and (3) [30].

The pseudo-first order

$$\log(q_e - q_t) = \log q_e - k_1 \frac{t}{2.303} \quad (2)$$

The pseudo-second order

$$\frac{t}{q_t} = \frac{1}{k_2 q_e^2} + \frac{t}{q_e} \quad (3)$$

q_t = the adsorbed mass per unit mass of adsorbent at time t (mg/g)
q_e = the adsorbed mass per unit mass of adsorbent at equilibrium (mg/g)
t = time (min)
k_1 = the rate constant for pseudo-first order adsorption (1/min)
k_2 = the rate constant for pseudo-second order adsorption (g/mg.min)

3. Results and Discussion

3.1 Wastewater, biochar, and manganese oxide-loaded biochar (MnO_x-Biochar) characteristics

The COD of two synthetic wastewater samples was 702 mg/L (WW-A) and 7,054 mg/L (WW-B). The pH was in the range of 6.60-6.67.

From the FTIR spectra of biochar (Figure 1), the broad peak at 3326 cm^{-1} represented the O-H stretching vibrations of pectin, cellulose, hemicellulose, and lignin left after pyrolysis. The peaks at 1564 cm^{-1} and 1400 cm^{-1} indicated the existence of the C=O and COO- stretching vibrations of pectin. The peak at 1033 cm^{-1} was assigned to the C-O stretching vibration. From the FTIR spectra of MnO_x-Biochar (Figure 1b), the peak at 611 cm^{-1} was attributed to Mn-O appearing in MnO_x-Biochar [26].

The pH where positive charges equaled negative charges on the surface of MnO_x-Biochar was approximately 7.05. Results from Brunauer Emmett Teller (BET)/gas adsorption analyser indicated that the surface area of biochar was higher after being modified with manganese oxide (Table 1). The pore volume and pore size on the MnO_x-Biochar surface was decreased due to the deposition of MnO_x in the pores. The results were related to Faheem *et al.* [26], who synthesized MnO_x-loaded biochar from rice husk.

The Mn concentrations in biochar and MnO_x-Biochar as determined by AAS were 0.001 mg/g and 1.252 mg/g, respectively. The experimental results confirmed that there was Mn in the MnO_x-Biochar structure.

3.2 Influence of initial pH

MnO_x-Biochar (2g/L) was applied to various pH-adjusted synthetic wastewater. Peroxydisulfate was added to the wastewater to obtain a concentration of 100 mM. The contact time was 180 min. For the study of the treatment with the adsorption process, sodium peroxydisulfate was not added. The results are shown in Figure 2.

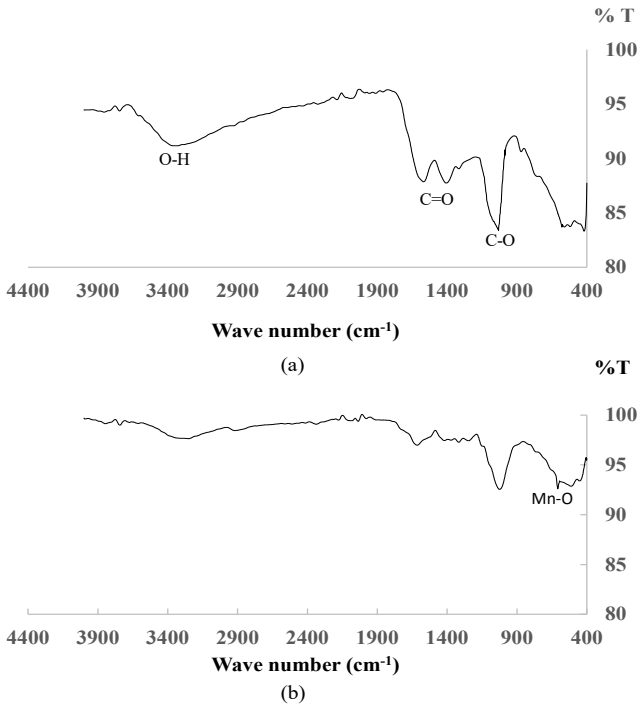

Figure 1. FTIR spectra of (a) Biochar and (b) MnO_x-Biochar

Table 1. Pore volume, pore size, and surface area of biochar and MnO_x-Biochar

	pore volume (cm^3/g)	pore size (nm)	surface area (m^2/g)
Biochar	0.078	1.53	85
MnO_x-Biochar	0.044	1.02	130

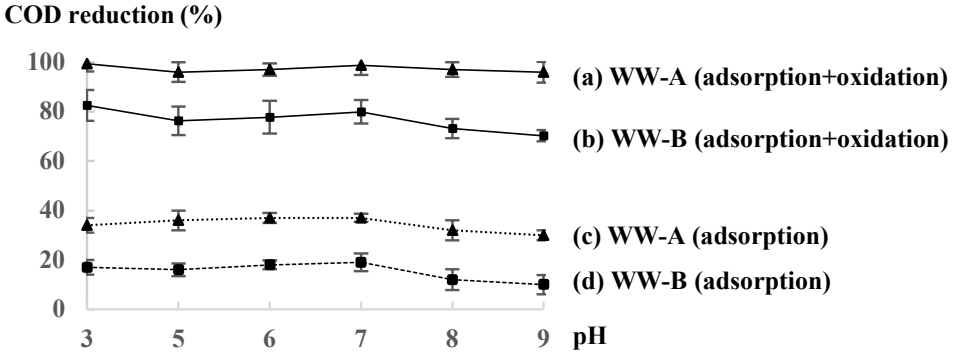

Figure 2. The COD reduction of wastewater when using various initial pH

Without persulfate, MnO_x-Biochar acted as an organic adsorbent. The organic adsorption efficiency for WW-A was higher than WW-B due to its lower concentration (Figure 2: graphs c and d). MnO_x-Biochar had a limited adsorption surface area and could not adsorb large amounts of contaminants, the higher the pH, the lower the organic adsorption. The point of zero charge of MnO_x-Biochar was 7.05, so when the pH was greater than 7.05, the surface charge of MnO_x-Biochar was positive, repelling the negative organic ions. The pH affected the adsorption process, but the adsorption efficiency was low. The organic adsorption efficiencies of WW-A and WW-B ranged from 30.0-37.1% and 10.3-19.1%.

The pH of the wastewater dropped to 2.48-2.55 after sodium peroxydisulfate was added. Peroxydisulfate oxidizes water forming sulfate ions (SO_4^{2-}), oxygen, and hydrogen ion (H^+) as shown in equation (4) [31]. The formation of hydrogen ions (H^+) can also occur as in equations (5) and (6).

$$2S_2O_8^{2-} + 2H_2O \longrightarrow 4SO_4^{2-} + O_2 + 4H^+ \quad (4)$$

$$S_2O_8^{2-} \longrightarrow 2SO_4^{\circ-} \quad (5)$$

$$SO_4^{\circ-} + H_2O \longrightarrow SO_4^{2-} + {}^\circ OH + H^+ \quad (6)$$

The presence of H^+ occured when persulfate was added, so the treatment efficiency was similar even though the initial pH of the wastewater was different. From the experimental results, it was concluded that the initial pH value of wastewater did not need to be adjusted prior to treatment. By comparing the results in curves a and c (Figure 2), the oxidation treatment efficiency was 60 to 66%. The efficiencies of treating WW-A and WW-B with the co-treatment process (adsorption and oxidation) were 96.0-98.9% and 74.3-82.5% (curves a and b), respectively.

3.3 Influence of MnO_x-Biochar dosage

Various MnO_x-Biochar dosages were applied to the synthetic wastewater without adjusting the pH of the wastewater. Peroxydisulfate was added to the wastewater to obtain a concentration of 100 mM. The treatment time was 180 min. For the study of the adsorption process, sodium peroxydisulfate was not added. The results are shown in Figure 3.

The contaminant adsorption efficiency in WW-A was higher than in WW-B due to the lower organic concentration in WW-A (Figure 3: curves c and d). Increasing the MnO_x-Biochar dosage resulted in a progressive increase of adsorption efficiency as the adsorption surface area increased. At the same time, increasing the MnO_x dosage increased the likelihood of persulfate catalysis (Figure 3: curves a and b). The reaction using MnO_x-Biochar as a catalyst is shown in equation (7).

$$M^{n+} + S_2O_8^{2-} \longrightarrow M^{(n+1)+} + SO_4^{\circ-} + SO_4^{2-} \quad (7)$$

The wastewater treatment efficiency with the co-treatment process (Figure 3: curves a and b) was higher than a single process (Figure 3: curves c and d). Optimum dosage of the co-treatment process was 2 g/L. The maximum efficacy of WW-A treatment was 98.9%. After the treatment, the Mn leaching was tested by AAS. There was no Mn found in wastewater after the treatment process.

3.4 Influence of contact time

Persulfate (100 mM) and MnO_x-Biochar (2 g/L) were added to wastewater. After allowing the reaction to proceed to different contact times, the COD of wastewater was measured. Figure 4 shows

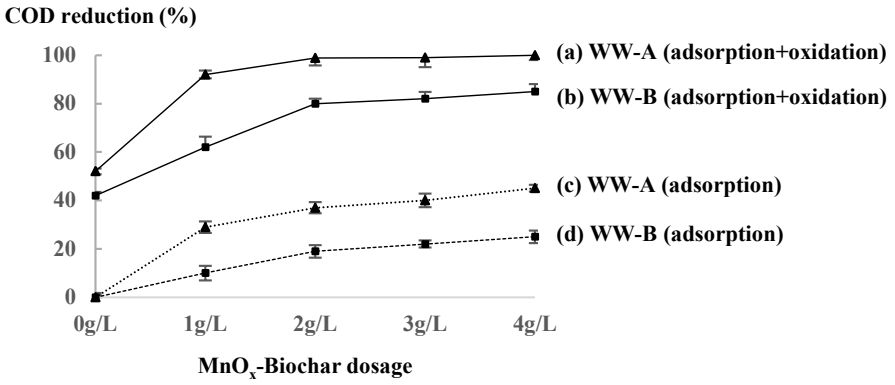

Figure 3. The COD reduction of wastewater when using various MnO_x-Biochar dosages

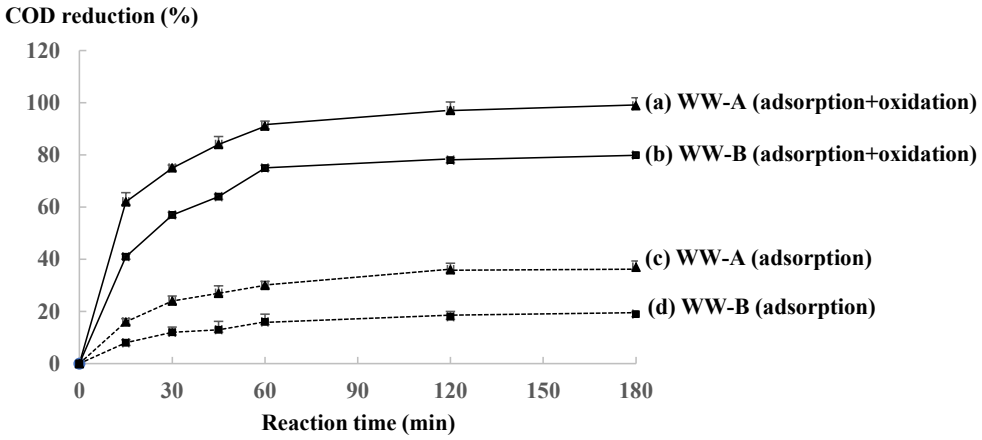

Figure 4. The COD reduction of wastewater at various contact times

the steepest slope occurred during the first 15 min of exposure due to the high level of COD in the wastewater during the initial treatment period. The k-values of WW-A and WW-B treatments during the first 15 min with the co-treatment process were 0.0647 min^{-1} and 0.0349 min^{-1}, respectively (Figure 4: curves a and b). After 15 min of treatment, the COD in wastewater had decreased. The k values of the WW-A and WW-B treatments had been reduced to 0.0242 min^{-1} and 0.0094 min^{-1}, respectively. An equilibrium was reached within 120 min of the reaction. However, in the experiment without the addition of persulfate, adsorption continued slowly after 120 min (Figure 4: curves c and d). The adsorption efficiencies at 120 min contact time for WW-A and WW-B were 36% and 18%, respectively (Figure 4: curves c and d). The efficiencies of treating the WW-A and WW-B via the co-treatment process (adsorption and oxidation) were 97% and 78%, respectively (curves a and b). The oxidation efficiencies for WW-A and WW-B treatments were 61% and 60%, respectively. For the adsorption process, the results of the kinetic model are shown in Figures 5 and 6.

From Figures 5 and 6, the best-fitting adsorption kinetic model for WW-A and WW-B were the pseudo-second order kinetic with the k values of 5.61×10^{-4} g/mg.min and 1.09×10^{-5} g/mg.min.

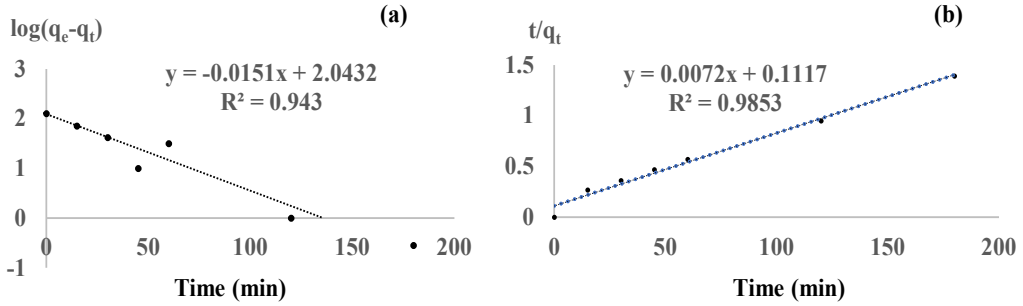

Figure 5. Adsorption kinetic model for WW-A (a) Pseudo-first order (b) Pseudo-second order

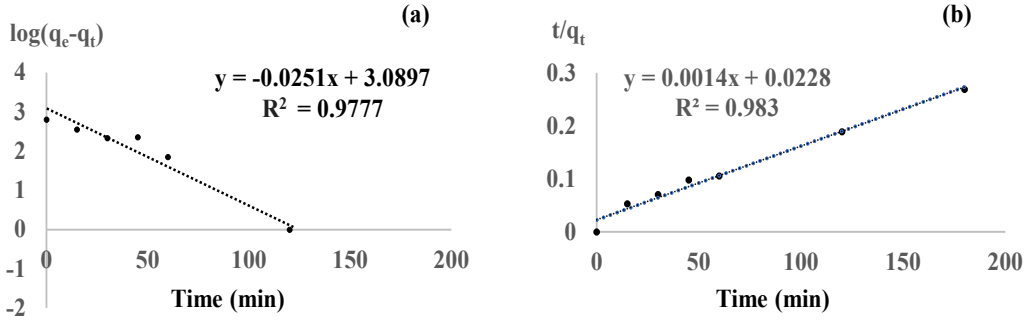

Figure 6. Adsorption kinetic model for WW-B (a) Pseudo-first order (b) Pseudo-second order

4. Conclusions

In this experiment, we recycled agricultural waste (corn cob) by converting it into biochar. Manganese oxide-loaded biochar (MnO_x-Biochar) was successfully synthesized as evidenced by the presence in the MnO_x-Biochar of a peak representing Mn-O stretching from FTIR analysis and the detection of Mn via AAS analysis. The surface area of the synthesized MnO_x-Biochar was higher than B, but the pore size and pore volume were smaller than B. Synthesis and treatment of low COD (702 mg/L) and high COD (7,054 mg/L) were performed. Without the addition of persulfate, MnO_x-Biochar adsorbed organic matter with low adsorption efficiency. By adding persulfate, MnO_x-Biochar could also stimulate the oxidation process of persulfate by 9-10%. When the initial pH of wastewater was higher than 7, the adsorption capacity of MnO_x-Biochar decreased. The initial pH of wastewater affected the adsorption process but did not affect the co-treatment process (oxidation and adsorption). The optimal dosage of MnO_x-Biochar was 2 g/L. An equilibrium was reached within 120 min of the reaction. The efficiencies of treating WW-A and WW-B with the co-treatment process (adsorption and oxidation) were 97% and 78%, respectively. The oxidation efficiencies for WW-A and WW-B were 61% and 60%, respectively. A pseudo-second order kinetic model well described the adsorption of organic matter in WW-A and WW-B by MnO_x-Biochar. Considering the co-treatment process, the k values of WW-A and WW-B treatment during the first 15 min were higher than after 15 min. Persulfate treatment has good efficacy; however, the water after treatment must be neutralized before it is released into the environment.

5. Acknowledgements

The authors are grateful to the School of Science, King Mongkut's Institute of Technology Ladkrabang, for providing funds, materials, and equipment.

References

[1] Office of Agricultural Economics, Ministry of Agriculture and Cooperatives, 2021. *Situations of Important Agricultural Products and Trends in 2022*. [online] Available at: https://www.oae.go.th/assets/portals/1/files/jounal/2565/trendstat2565-Final-Download.pdf. (in Thai)

[2] Grace, M.A., Clifford, E. and Healy, M.G., 2016. The potential for the use of waste products from a variety of sectors in water treatment processes. *Journal of Cleaner Production*, 137, 788-802.

[3] Department of Energy Business, Ministry of Energy, 2021. *List of fuel traders*. [online] Available at: https://www.doeb.go.th/info/info_operat_fuel.php. (in Thai)

[4] Sarmadi, M., Zarei, A.A., Ghahrchi, M., Sepehrnia, B., Meshkinian, A., Moein, H., Nakhaei, S. and Bazrafshan, E., 2021. Carwash wastewater characteristics - a systematic review study. *Desalination and Water Treatment*, 225, 112-148.

[5] Rai, R., Sharma, S., Gurung, D.B., Sitaula, B.K. and Shah, R.D.T., 2019. Assessing the impacts of vehicle wash wastewater on surface water quality through physio-chemical and benthic macroinvertebrates analyses. *Water Science*, 40, 39-49.

[6] El-Ashtoukhy, E.Z., Amin, N.K. and Fouad, Y.O., 2015. Treatment of real wastewater produced from mobil carwash station using electrocoagulation technique. *Environmental Monitoring and Assessment*, 187, 628-638.

[7] Pinto, A.C.S., Grossi, L.B., Melo, R.A.C., Assis, T.M., Ribeiro, V.M., Amaral, M.C.S. and Figueiredo, K.C.S., 2017. Carwash wastewater treatment by micro and ultrafiltration membranes: Effects of geometry, pore size, pressure difference and feed flow rate in transport properties. *Journal of Water Process Engineering*, 17, 143-148.

[8] Moazzem, S., Wills, J., Fan, L., Roddick, F. and Jegatheesan, V., 2018. Performance of ceramic ultrafiltration and reverse osmosis membranes in treating carwash wastewater for reuse. *Environmental Science and Pollution Research*, 25, 8654-8668.

[9] Mallick, S.K. and Chakraborty, S., 2019. Bioremediation of wastewater from automobile service station in anoxic-aerobic sequential reactors and microbial analysis. *Chemical Engineering Journal*, 361, 982-989.

[10] Davarnejad, R., Sarvmeili, K. and Sabzehei, M., 2020. Car wash wastewater treatment using an advanced oxidation process: A rapid technique for the COD reduction of water pollutant sources. *Journal of the Mexican Chemical Society*, 63(4), 164-175.

[11] Deng, Y. and Zhao, R., 2015. Advanced oxidation processes (AOPs) in wastewater treatment. *Current Pollution Reports*, 1, 167-176.

[12] Klamerth, N., Malato, S., Agüera, A. and Fernández-Alba, A., 2013. Photo-Fenton and modified photo-Fenton at neutral pH for the treatment of emerging contaminants in wastewater treatment plant effluents: A comparison. *Water Research*, 47(2), 833-840.

[13] Hunge, Y., Yadav, A., Khan, S., Takagi, K., Suzuki, N., Teshima, K., Terashima, C. and Fujishima, A., 2020. Photocatalytic degradation of bisphenol A using titanium dioxide@nano diamond composites under UV light illumination. *Journal of Colloid and Interface Science*, 582, 1058-1066.

[14] Iboukhoulef, H., Amrane, A. and Kadi, H., 2016. Removal of phenolic compounds from olive mill wastewater by a Fenton-like system H_2O_2/Cu (II)—Thermodynamic and kinetic modelling. *Desalination and Water Treatment*, 57, 1874-1879.

[15] Heck, K.N., Wang, Y., Wu, G., Wang, F., Tsai, A-L., Adamsond, D.T. and Wong, M.S., 2019. Effectiveness of metal oxide catalysts for the degradation of 1,4-dioxane. *RSC Advances*, 9(46), 27042-27049.

[16] Huang C.P. and Huang, Y.H., 2008. Comparison of catalytic decomposition of hydrogen peroxide and catalytic degradation of phenol by immobilized iron oxides. *Applied Catalysis A: General*, 346(1), 140-148.

[17] Lee, Y.C., Lo, S.L., Kuo, J. and Huang, C.P., 2013. Promoted degradation of perfluorooctanic acid by persulfate when adding activated carbon. *Journal of Hazardous Materials*, 261, 463-469.

[18] Lee, J., Gunten, U.V. and Kim, J.H., 2020. Persulfate-based advanced oxidation: Critical assessment of opportunities and roadblocks. *Environmental Science & Technology*, 54(6), 3064-3081.

[19] Hua, M., Zhang, S., Pan, B., Zhang, W., Lv, L. and Zhang, Q., 2012. Heavy metal removal from water/wastewater by nanosized metal oxides: A review. *Journal of Hazardous Materials*, 211, 317-331.

[20] Matzek, L.W. and Carter, K.E., 2016. Activated persulfate for organic chemical degradation: A review. *Chemosphere*, 151, 158-178.

[21] Aher, A., Papp, J., Colburn, A., Wan, H., Hatakeyama, E., Prakash, P., Weaver, B. and Bhattacharyya, D., 2017. Naphthenic acids removal from high TDS produced water by persulfate mediated iron oxide functionalized catalytic membrane, and by nano-filtration. *Chemical Engineering Journal*, 327, 573-583.

[22] Ghanbari, F. and Moradi, M., 2017. Application of peroxymonosulfate and its activation methods for degradation of environmental organic pollutants: Review. *Chemical Engineering Journal*, 310, 41-62.

[23] Jia, D., Hanna, K., Mailhot, G. and Brigante, M., 2021. A Review of manganese (III) (oxyhydr) oxides use in advanced oxidation processes. *Molecules*, 26, 5748-5768.

[24] Zhao, Q., Mao, Q., Zhou, Y., Wei, J., Liu, X., Yang, J., Luo, L., Zhang, J., Chen, H., Chen, H. and Tang, L., 2017. Metal-free carbon materials-catalyzed sulfate radical-based advanced oxidation processes: A review on heterogeneous catalysts and applications. *Chemosphere*, 189, 224-238.

[25] Fan, Z., Zhang, Q., Li, M., Sang, W., Qiu, Y. and Xie, C., 2019. Activation of persulfate by manganese oxide-modified sludge-derived biochar to degrade Orange G in aqueous solution. *Environmental Pollutants and Bioavailability*, 31(1), 70-79.

[26] Faheem, Yu, H., Liu, J., Shen, J., Sun, X., Li, J. and Wang, L., 2016. Preparation of MnO_x-loaded biochar for Pb^{2+}removal: Adsorption performance and possible mechanism. *Journal of the Taiwan Institute of Chemical Engineers*, 66, 313-320.

[27] US EPA, 1978. *Method 410.3: Chemical Oxygen Demand by Titration*. [online] Available at: https://www.epa.gov/sites/default/files/2015-08/documents/method_410-3_1978.pdf.

[28] US EPA, 1996. *Method 3050b: Acid Digestion of Sediments, Sludges and Soil/SW-846*. [online] Available at: https://www.epa.gov/sites/default/files/2015-06/documents/epa-3050b. pdf.

[29] Ahmed, M.B., Zhou, J.L., Ngo, H.H. and Chen, W.G.M., 2016. Progress in the preparation and application of modified biochar for improved contaminant removal from water and wastewater. *Bioresource Technology*, 214, 836-851.

[30] Yakout, S.M. and Elsherif, E., 2010. Batch kinetics, isotherm and thermodynamic studies of adsorption of strontium from aqueous solutions onto low cost rice-straw based carbons. *Carbon-Science and Technolology*, 3, 144-153.

[31] Lee, C., Kim, H.H. and Park, N.B., 2018. Chemistry of persulfates for the oxidation of organic contaminants in water. *Membrane Water Treatment*, 9(6), 405-419.